RSC Advances

PAPER

View Article Online
View Journal | View Issue

Cite this: *RSC Adv.*, 2022, **12**, 33525

Design, synthesis, and biological evaluation of novel bioactive thalidomide analogs as anticancer immunomodulatory agents†

Anas Ramadan Kotb,[a] Dina A. Bakhotmah,*[b] Abdallah E. Abdallah,[a] Hazem Elkady,[a] Mohammed S. Taghour,[a] Ibrahim. H. Eissa*[a] and Mohamed Ayman El-Zahabi*[a]

Cancer is still a dangerous disease with a high mortality rate all over the world. In our attempt to develop potential anticancer candidates, new quinazoline and phthalazine based compounds were designed and synthesized. The new derivatives were built in line with the pharmacophoric features of thalidomide. The new derivatives as well as thalidomide were examined against three cancer cell lines, namely: hepatocellular carcinoma (HepG-2), breast cancer (MCF-7) and prostate cancer (PC3). Then the effects on the expression levels of caspase-8, VEGF, NF-κB P65, and TNF-α in HepG-2 cells were evaluated. The biological data revealed the high importance of phthalazine based compounds (**24a–c**), which were far better than thalidomide with regard to the antiproliferative activity. **24b** showed IC_{50} of 2.51, 5.80 and 4.11 μg mL^{-1} compared to 11.26, 14.58, and 16.87 μg mL^{-1} for thalidomide against the three cell lines respectively. **24b** raised caspase-8 level by about 7 folds, compared to 8 folds reported for thalidomide. Also, VEGF level in HepG-2 cells treated with **24b** was 185.3 pg mL^{-1}, compared to 432.5 pg mL^{-1} in control cells. Furthermore, the immunomodulatory properties were proven to **24b**, which reduced TNF-α level by approximately half. At the same time, NF-κB P65 level in HepG-2 cells treated with **24b** was 76.5 pg mL^{-1} compared to 278.1 and 110.5 pg mL^{-1} measured for control cells and thalidomide treated HepG-2 cells respectively. Moreover, an *in vitro* viability study against Vero non-cancerous cell line was investigated and the results reflected a high safety profile of all tested compounds. This work suggests **24b** as a promising lead compound for development of new immunomodulatory anticancer agents.

Received 1st October 2022
Accepted 14th November 2022

DOI: 10.1039/d2ra06188k

rsc.li/rsc-advances

1. Introduction

In the last few decades, there has been a tremendous amount of effort and progress in cancer treatment. However, cancer is still a disease with an increasingly high mortality rate all over the world.[1] Many challenges have been reported clinically, including resistance of cancer to the used drugs, which leads to failure of the treatment.[2–4] In addition to that, the toxicity of many anticancer drugs is not limited to cancer cells.[5] As a result, severe and serious toxic effects were reported[6,7] as well as difficulties in optimizing the drug regimen.[8] These two main problems were taken into account in this study which aimed to develop anticancer candidates with potential low resistance rate and few side effects.[9]

In our journey to find a suitable lead, thalidomide emerged as a lead with many significant criteria. Aside from teratogenicity, thalidomide was found to exhibit few side effects.[10] It was modified to give what is known as immunomodulatory drugs (IMiDs), such as lenalidomide and pomalidomide, that were approved for cancer treatment.[11–13] The significant anticancer effects of thalidomide and the IMiDs have been proven to involve different targets and several mechanisms, which include immunomodulatory action. Vascular endothelial growth factor (VEGF) and hence angiogenesis were reported to be inhibited by these drugs.[14] Also, the apoptosis rate and cell cycle arrest were increased along with the elevation of caspase-8 levels.[14] Furthermore, the immunomodulatory effects that include co-stimulation of T-cells, inhibition of proinflammatory cytokines such as tumor necrosis factor-alpha (TNF-α), interleukin-6 (IL-6), IL-1, IL-12. In addition to nuclear factor kappa B (NFκB) inhibition.[14] On the other hand, the levels of the anti-inflammatory cytokines were elevated. The elevated cytokines include interferon-gamma (IFN-γ) and IL-10, IL-2.[11,15–19] Thalidomide's immunomodulatory properties account for its efficacy in various autoimmune and inflammatory diseases.[20,21] Based on these characteristics, we suggest that thalidomide

[a]*Pharmaceutical Medicinal Chemistry & Drug Design Department, Faculty of Pharmacy (Boys), Al-Azhar University, Cairo, 11884, Egypt. E-mail: malzahaby@azhar.edu.eg; Ibrahimeissa@azhar.edu.eg*

[b]*Department of Chemistry, Faculty of Science, King Abdulaziz University, Jeddah, Saudi Arabia. E-mail: dbakhotmah@kau.edu.sa*

† Electronic supplementary information (ESI) available. See DOI: https://doi.org/10.1039/d2ra06188k

modification may afford new effective and safe candidates with a low resistance rate.

Thalidomide structural modifications have resulted in many effective anticancer analogs such as lenalidomide, pomalidomide,[22] and avadomide (CC-122).[23] Thalidomide was approved for treatment of acute ENL in 1998 and for treatment of multiple myeloma (MM) in 2006.[24] Lenalidomide was found to be a more potent TNF-α inhibitor than thalidomide.[25] In 2006, it received FDA approval for treatment of MM.[26] Pomalidomide showed more significant results than lenalidomide in both inhibition of TNF-α and stimulation of IL-2.[27] In 2013, it was approved by FDA for treatment of MM.[28] Avadomide exhibited potent antiproliferative, anti-angiogenic and immunomodulatory activities.[29] It was proven to be effective in treatment of MM, diffuse large B-cell lymphoma (DLBCL) and solid tumors.[23]

The structural modification of thalidomide that involved the replacement of the phthalimido moiety by quinazoline nucleus afforded avadomide.[30] Quinazoline containing candidates revealed potent inhibition to NF-κB,[31] TNF-α, IL-6, and IL1β,[32–34] antiproliferative[35] and immunomodulatory activities[36] along with induction of apoptosis and elevation of caspase levels.[37] The compounds based on phthalazine, a bio-isostere of quinazoline, showed similar properties which included TNF-α and NF-κB inhibition,[38] antiproliferative,[39] apoptosis induction[40] and antiangiogenic effect.[41]

1.1. Rationale of molecular design

It is clear that thalidomide has many targets involved in the expression of its high efficacy in cancer, autoimmune and inflammatory diseases. As a result, analyzing the binding interactions to one or two targets does not provide an explanation for all the biological effects reported for thalidomide. But analyzing the chemical structure of thalidomide may be a better way to design new candidates with similar properties. Hence, the ligand-based design approach has been followed in this study. The molecular structure of thalidomide as a lead compound can be analyzed into four main regions as illustrated in Fig. 1. Four pharmacophoric features are identified as follows: (1) a flat hetero aromatic ring, (2) a spacer, (3) a hydrogen bond forming region, (4) a hydrophobic moiety.

Herein, we carried out modifications on the analyzed four regions. Firstly, the phthalimide moiety was replaced with two other bio-isostere heteroaromatic nuclei; quinazoline and phthalazine. It was reported that quinazoline was a significant alternative to phthalimide and afforded the highly effective avadomide molecule. Secondly, it is noticed that the rotation of the sigma bond between glutarimide moiety and phthalimide nucleus of thalidomide is almost restricted. We aimed to increase the flexibility by having one or two NH groups which will allow more flexibility of the attached planar

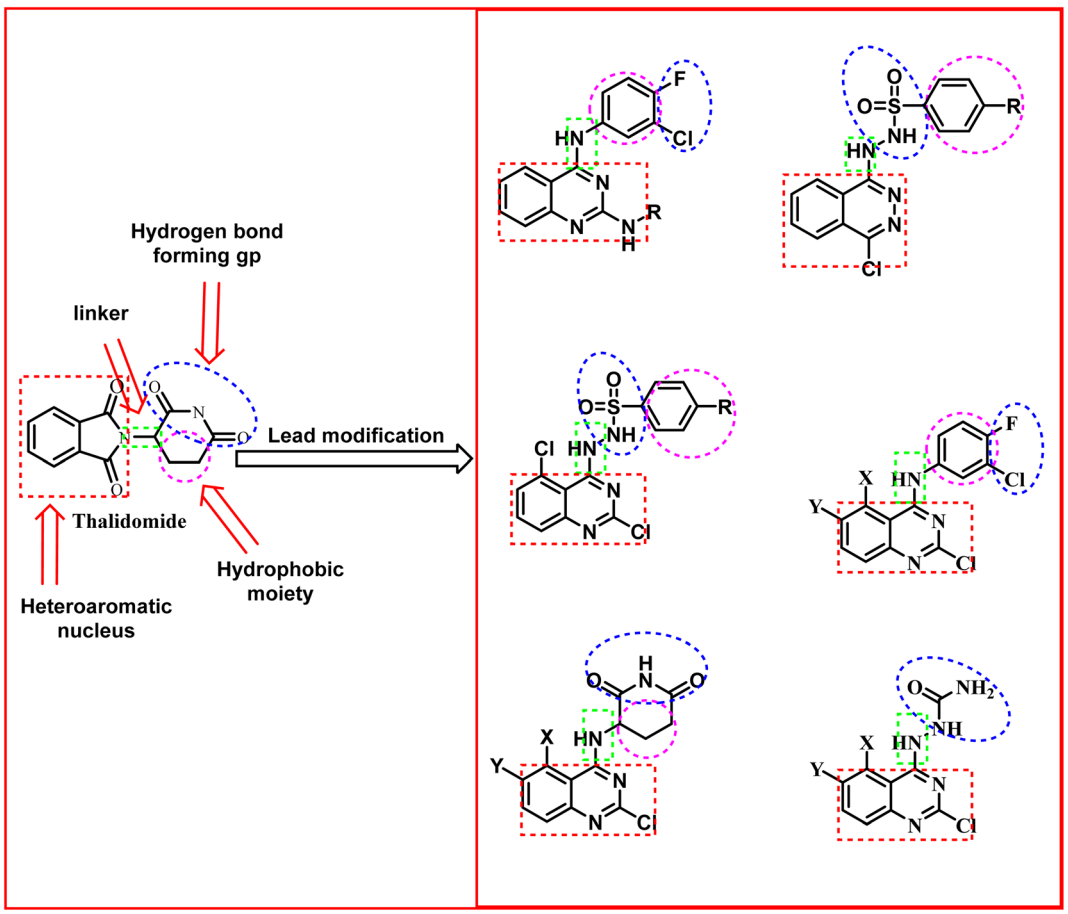

Fig. 1 Illustration for the rationale of the design.

benzenesulfonyl, the clororfluroranilide moieties or the puckered glutarimide ring or ring open modification of the semicarbazide moiety. Consequently, such possible variations may result in biological variations due to possible variations of the way of binding to the target binding sites as shown in Fig. 1. Thirdly, the hydrogen bond forming group was designed to include imide, urea, sulfamoyl, and even hydrogen bond forming halogens *e.g.*, fluoro and chloro. Finally, aliphatic and aromatic groups were constructed to examine which would be the most effective as a hydrophobic moiety in terms of thalidomide activities.

2. Results and discussion

2.1. Chemistry

For synthesis of the target compounds, reactions sequence is clarified in Schemes 1–3. Initially, quinazoline-2,4(1*H*,3*H*)-dione **3** was prepared by fusion of anthranilic acid **1** with urea **2** according to the reported methods.[42] Next, heating of **3** with phosphorus oxychloride in the presence of Et_3N for 7 h afforded the dichloro derivative **4**.[43] The produced 2,4-dichloroquinazoline **4** was refluxed with 3-chloro-4-fluoroaniline **5** in isopropyl alcohol in the presence of two mole equivalents of Et_3N to produce the final target compound **6**. Refluxing two-mole equivalents of methyl and ethyl amine with compound **6** in acetonitrile gave compounds **7a,b** respectively (Scheme 1). The structures of compounds **6** and **7a,b** were verified by elemental analyses and spectral data. The IR spectra of these compounds revealed the presence of NH absorption bands at a range of 3380–3277 cm^{-1}. Moreover, the ^1H NMR spectra of compound **6** showed peak at 10.26 ppm due to NH. On the other hand, the ^1H NMR spectra of compounds **7a,b** showed deshielded peaks at a range of 8.30 to 9.5 ppm corresponding to the two NHs. Additionally, the aliphatic protons appeared at a range of 1.02 to 3.48 ppm.

In Scheme 2, the starting materials **9a,b** were reported to be prepared by fusion of urea with 5-chloroanthranilic acid **8a** or 6-chloroanthranilic acid **8b**, respectively. Chlorination of the produced quinazoline-2,4-dione derivatives **9a,b** was achieved by refluxing in $POCl_3$ in the presence of *N*,*N*-dimethyl aniline (DMA) following the reported procedure.[44] The target compounds **11a,b** were finalized by refluxing 2,4,5-trichloro-1,2,3,4-tetrahydroquinazoline **10a** and/or 2,4,6-trichloro-1,2,3,4-tetrahydroquinazoline **10b** with 3-chloro-4-fluoroaniline **5** in isopropyl alcohol in the presence of Et_3N. IR spectra revealed the presence of NH absorption bands at 3419 and 3381 cm^{-1}. On the other hand, the ^1H NMR spectra of compounds **11a,b** showed deshielded peaks for the NH protons at a range of 10.31 to 9.87 ppm. In the meantime, compounds **13a,b** were furnished by refluxing the appropriate 2,4-dichloroquinazoline derivatives **10a,b** with 3-aminopiperidine-2,6-dione HCl **12** under basic conditions. Also, under the same condition reactions, compounds **15a,b** was produced by reaction of **10a,b** with semicarbazide HCl **14**. Treatment of 2,4,5-trichloroquinazoline **10a** with excess hydrazine hydrate **16** in absolute ethanol afforded 2,5-dichloro-4-hydrazinylquinazoline **17**.[45] Finally, synthesis of compounds **19a,b** was attained in good yields by dropwise addition of the appropriate benzenesulfonyl chloride **18a,b** to a mixture of 2,5-dichloro-4-hydrazinylquinazoline **17** and Et_3N in DMF in ice salt bath. The IR spectra of these compounds were characterized by appearance of characteristic bands of the two NH groups at 3397–3306 cm^{-1} and very characteristic bands of SO_2 group at a range of 1166–1163 cm^{-1}. On the other hand, the ^1H NMR

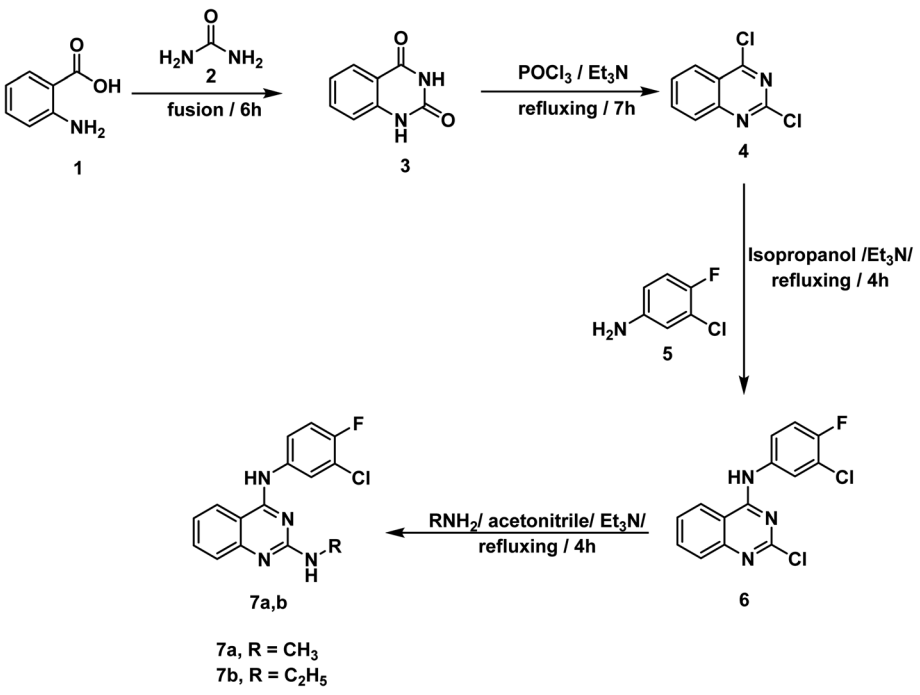

Scheme 1 General procedure for preparation of target compounds 6 and 7a,b.

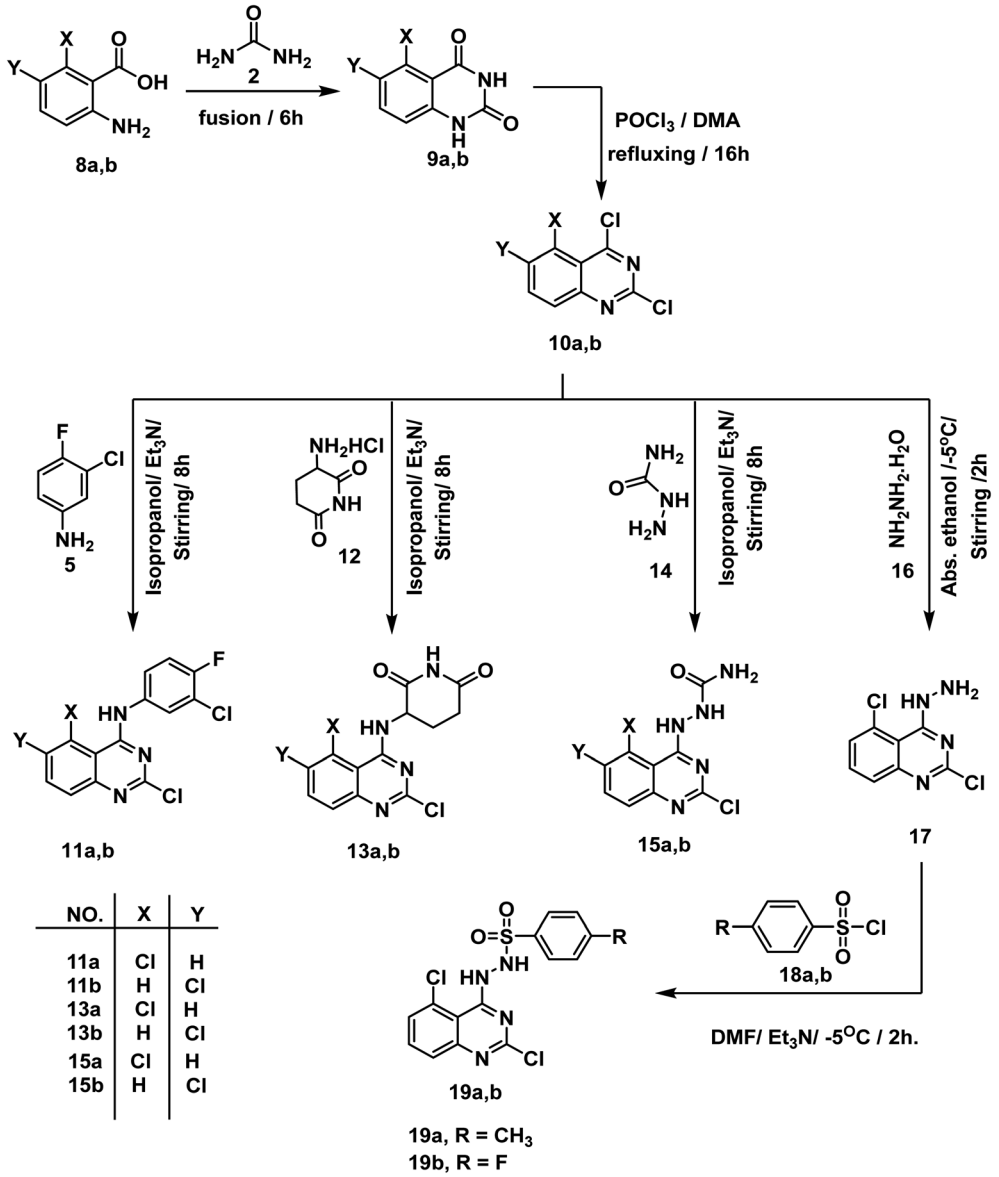

Scheme 2 General procedure for preparation of target compounds **11a,b**, **13a,b**, **15a,b**, and **19a,b**.

spectrum of **19a** showed peaks at 10.04 and 7.82 ppm due to sulfonhydrazide moiety while compound **19b** showed peaks at 10.24, 7.97 ppm.

2,3-Dihydrophthalazine-1,4-dione **21** was prepared by condensation of equimolar amounts of phthalic anhydride **20** and hydrazine hydrate **16** in absolute ethanol, according to a reported procedure[46] as illustrated in Scheme 3. Refluxing of **21** in $POCl_3$ afforded 1,4-dichlorophthalazine **22**, which was then treated with an excess of hydrazine hydrate **16** to give 1-chloro-4-hydrazinylphthalazine **23** as shown in Scheme 3. Finally, the target compounds **24a–c** were obtained by addition of an appropriate benzenesulfonyl chloride **18a–c** dropwise to a cooled solution of **23** in DMF. The ^{1}H NMR spectra of **24a–c** showed peaks at about 11.75 and 9.44 ppm due to sulfonhydrazide moiety.

2.2. Biological testing

2.2.1. *In vitro* anti-proliferative activity. The new candidates were evaluated against three cancer cell lines, namely: hepatocellular carcinoma (HepG-2), breast cancer (MCF-7) and prostate cancer (PC3). The concentrations that caused 50% growth inhibition (IC_{50}) were calculated. Thalidomide was used as a positive reference. The data obtained are presented in Table 1.

It is noticeable that the **24a–c** compounds, which are based on the phthalazine core carrying the sulfonhydrazide moiety, showed the best antiproliferative results. Such compounds are, in fact, significantly better than thalidomide *versus* the selected cancer cell lines. The most significant candidate was **24b**, which showed IC_{50} of 2.51, 5.80 and 4.11 μg mL^{-1} compared to 11.26, 14.58, and 16.87 μg mL^{-1} for thalidomide against the three cell

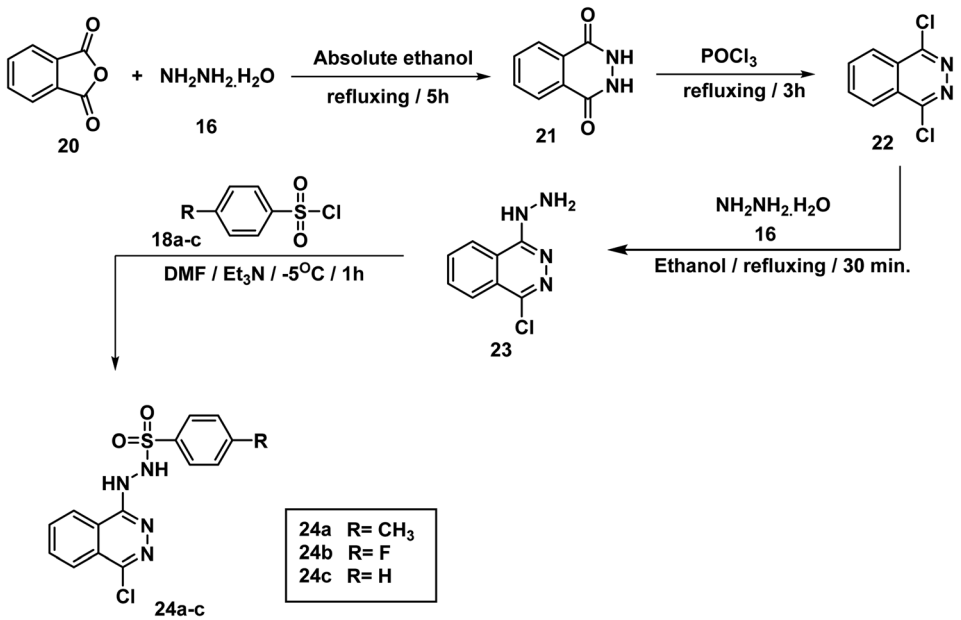

Scheme 3 General methods for preparation of the new derivatives **24a–c**.

Table 1 Anti-proliferative activities of the target compounds against HepG-2, PC3 and MCF-7 cell lines

	In vitro cytotoxicity IC_{50}[a] (μg mL^{-1})		
Comp	HepG-2	MCF-7	PC3
6	74.81 ± 4.1	81.52 ± 4.2	84.96 ± 4.7
7a	40.50 ± 2.8	28.13 ± 2.1	47.20 ± 2.8
7b	11.68 ± 0.8	9.45 ± 0.9	15.48 ± 1.3
11a	77.24 ± 4.2	86.14 ± 4.4	91.26 ± 4.9
11b	38.74 ± 2.8	45.91 ± 3.0	51.20 ± 3.5
13a	46.32 ± 3.1	35.29 ± 2.4	54.31 ± 3.0
13b	59.01 ± 3.3	29.33 ± 2.3	38.36 ± 3.1
15a	24.51 ± 2.0	17.33 ± 1.3	26.08 ± 2.0
15b	16.18 ± 1.4	9.87 ± 0.9	13.79 ± 1.2
19a	19.07 ± 1.5	12.76 ± 1.0	21.48 ± 1.6
19b	28.92 ± 2.2	20.48 ± 1.5	32.71 ± 2.3
24a	3.87 ± 0.2	6.07 ± 0.7	8.63 ± 0.6
24b	2.51 ± 0.1	5.80 ± 0.4	4.11 ± 0.3
24c	7.96 ± 0.5	8.12 ± 0.7	14.92 ± 1.1
Thalidomide	11.26 ± 0.54	14.58 ± 0.57	16.87 ± 0.7

[a] Three independent experiments were performed for each concentration.

lines respectively. Compound **24a** came in second with IC_{50} of 3.87, 6.07, and 8.63 μg mL^{-1} respectively. The third was compound **24c**, which showed an IC_{50} of 7.96, 8.12, and 14.92 μg mL^{-1} respectively.

The best quinazoline derivative was **7b**, in which the quinazoline nucleus was attached to chlorofluoroanilide group at position 4 and ethyl amino group at position 2. It showed results better than thalidomide against both MCF-7 and PC3, and comparable to that of thalidomide against HepG-2. It is also noticed that compound **15b** was stronger than thalidomide against MCF-7 and PC3, but weaker than it against HepG-2. Compounds **19a**, **15a**, and **19b** revealed moderate activities. It was found clear that HepG-2 was the most sensitive cancer cell line for the most promising candidates (**24a–c**). Accordingly, HepG-2 cell line was selected for further evaluation. Two compounds were selected for such evaluation; phthalazine based **24b** (the most effective candidate) and **7b** (the most promising quinazoline based derivative).

2.2.2. Structure activity relationship. Observing the results of biological testing (*in vitro* anti-proliferative activity), we could determine valuable data about the structure–activity relationships.

Regarding quinazoline containing derivatives, comparing the cytotoxic activity of compounds **11b**, **13b**, and **15b** (incorporating 2,6-dichloroquinazoline moiety) with compounds **11a**, **13a**, and **15a** (incorporating 2,5-dichloroquinazoline moiety) indicated that 2,6-dichloroquinazoline moiety is more advantageous than 2,5-dichloroquinazoline moiety for cytotoxic activity against all cell lines. Moreover, comparing the activity of compounds **15a** and **15b** having semicarbazide moiety with compounds **13a** and **13b** having glutarimide moiety indicated that semicarbazide moieties are more beneficial for activity. Regarding 2-chloroquinazoline derivatives **6**, **7a**,**b**, it was noticed that replacement of chlorine atom at position-2 with methylamine increased the cytotoxic activity against all cell lines. However, replacement of methylamine with ethylamine increased the cytotoxic activity against all cell lines as well. With regard to phthalazine containing derivatives, comparing the activity of compound **24a** (in which 4-methylbenzenesulfonohydrazide moiety is incorporated) and compound **24b** (in which 4-fluorobenzenesulfonohydrazide moiety is incorporated) with compound **24a** (in which benzenesulfonohydrazide moiety is incorporated), revealed that substituted moieties are more potent than unsubstituted one. In the meantime, comparing the activity of compound **24c** (incorporating 4-fluorobenzenesulfonohydrazide moiety) with

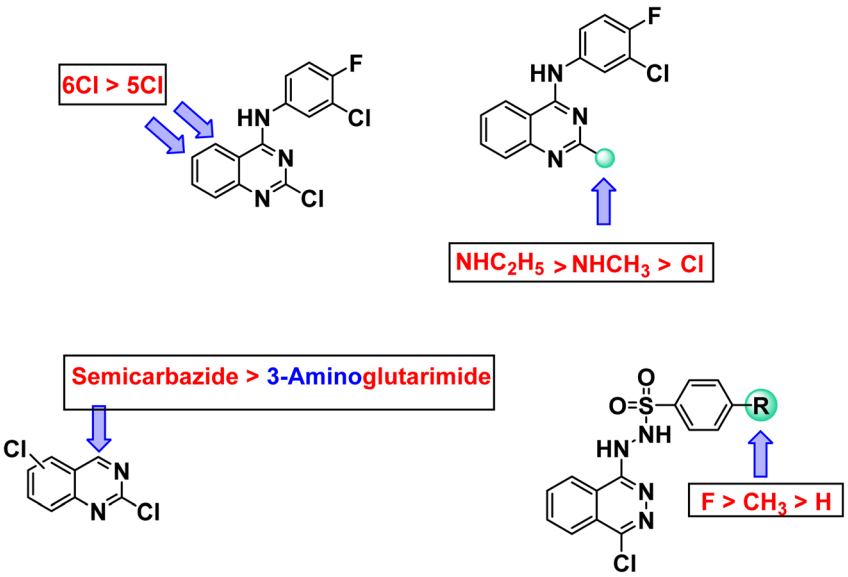

Fig. 2 Structure–activity relationship based on *in vitro* anti-proliferative activity.

compound **24b** (incorporating 4-methylbenzenesulfonohydrazide moiety), exhibited that the electron withdrawing group is more preferred biologically than electron donating one (Fig. 2).

2.2.3. *In vitro* protein expression assay. Compounds **24b** and **7b**, along with thalidomide as a positive reference, were tested in HepG-2 cells for their effects on the expression levels of caspase-8 and VEGF.

2.2.3.1. The effect on the expression level of caspase-8. It was found that compound **24b** was able to increase caspase-8 level in HepG-2 cells by about 7 folds, compared to 8 folds reported for thalidomide. While **7b** revealed a threefold increase in caspase-8 level as shown in Table 2.

2.2.3.2. The effect on the expression level of vascular endothelial growth factor (VEGF). The data presented in Table 2 show that compound **24b** reduced the level of VEGF to less than half of that of control cells. HepG-2 cells treated with **24b** revealed VEGF level of 185.3 pg mL^{-1}, compared to 432.5 pg mL^{-1} calculated for control cells. Additionally, **7b** reduced VEGF level in HepG-2 cells by about half (218.5 pg mL^{-1}). On the other hand, VEGF level in HepG-2 cells treated with thalidomide was found to be 153.2 pg mL^{-1}.

2.2.4. *In vitro* immunomodulatory assay. The effects of **24b** and **7b**, as well as thalidomide, on the expression levels of NF-κB P65 and TNF-α in HepG-2 were studied further.

2.2.4.1. The effect on NF-κB P65 expression level. The obtained data indicated that the impact of **24b** on NF-κB P65 was much better than thalidomide. It can be seen that NF-κB P65 level in HepG-2 cells treated with **24b** was 76.5 pg mL^{-1} compared to 278.1 and 110.5 pg mL^{-1} measured for control HepG-2 cells and thalidomide treated HepG-2 cells respectively. At the same time compound **7b** showed a result that was almost comparable to that of thalidomide (Table 2).

2.2.4.2. The effect on TNF-α expression level. The data presented in Table 2 shows that both **24b** and **7b** reduced TNF-α levels in HepG-2 cells by about half. TNF-α levels were reduced from 162.5 pg mL^{-1} in control cells to 82.5 and 79.3 pg mL^{-1} under the effects of **24b** and **7b** respectively. On the other hand, the level in cells treated with thalidomide was 53.1 pg mL^{-1}.

2.2.5. Cytotoxicity against Vero cells and selectivity index. The most promising candidates (**7b** and **24b**) were investigated for their safety patterns against normal cell line (Vero cells). Using MTT assay, compounds **7b** and **24b** showed IC_{50} values of 163.61 and 161.12 μg mL^{-1}. Such values were very high in comparison to the corresponding values on cancer cell lines, which reflect the high *in vitro* safety profile of the tested members towards non-cancerous cell line (Table 3).

The selectivity index (SI) of a particular compound is the ratio of its toxic concentration against the effective concentration (SI = IC_{50} on non-cancer cell/IC_{50} on cancer cell).[47] From the results presented in Table 3, the tested compounds showed very high SI against the cancer cell lines. Interestingly, compound **24b** showed the highest SI values of 65.18 and 39.80 against the HepG2, and PC3 cell lines, respectively. Compound

Table 2 The effect of the selected candidates and thalidomide on the levels of caspase-8, VEGF, NFκB and TNF-α

Comp. no.	CASPASE-8 (ng mL^{-1})	VEGF (pg mL^{-1})	NFκB P65 (pg mL^{-1})	TNF-α (pg mL^{-1})
24b	6.9	185.3	76.5	82.5
7b	3.2	218.5	113.7	79.3
Control	1.08	432.5	278.1	162.5
Thalidomide	8.3	153.2	110.5	53.1

Table 3 IC_{50} values of the tested compounds against Vero cell line and their selectivity index (SI) against different cancer cell lines

Compounds	Cytotoxicity against Vero (IC_{50} μg mL^{-1})	Selectivity index (SI)		
		HepG-2[a]	MCF-7[b]	PC3[c]
7b	163.61 ± 1.12	13.78	17.04	10.40
24b	161.12 ± 1.42	65.18	8.59	39.80

[a] SI = cytotoxicity against Vero cells/cytotoxicity against HepG-2 cell line. [b] SI = cytotoxicity against Vero cells/cytotoxicity against MCF-7 cell line. [c] SI = cytotoxicity against Vero cells/cytotoxicity against PC3 cell line.

Table 4 Physicochemical properties of the tested members

Comp	Lipinski rules				Veber's rules	
	HBD	HBA	M_{wt}	log *P*	Rotatable bonds	TPSA
6	1	3	308.138	5.202	2	37.81
7a	2	4	302.734	4.677	3	49.84
7b	2	4	316.761	5.025	4	49.84
11a	1	3	342.583	5.867	2	37.81
11b	2	5	325.15	2.49	2	83.97
13a	3	4	272.091	2.379	2	92.93
13b	1	3	342.583	5.867	2	37.81
15a	2	5	325.15	2.49	2	83.97
15b	3	4	272.091	2.379	2	92.93
19a	2	5	383.252	4.443	4	92.36
19b	2	5	387.216	4.162	4	92.36
24a	2	5	348.807	3.529	4	92.36
24b	2	5	352.771	3.248	4	92.36
24c	2	5	334.781	3.043	4	92.36
Thalidomide	1	4	258.229	0.097	1	83.55

7b showed SI values of 13.78, 17.04, and 10.40 against the HepG2, MCF-7, and PC3 cell lines, respectively.

2.3. *In silico* investigation

2.3.1. Lipinski's rule of five and Veber's rule. According to Veber's and Lipinski's rule of five, an *in silico* computational analysis of the tested candidates was done to ascertain their physicochemical properties.

The results presented in Table 4 showed that the tested compounds showed no contravention of Lipinski's and Veber's rules and hence display a drug-like molecular nature. In details, the partition coefficient (log *P*) values were less than 5 except compounds **6**, **7b**, and **11a**, and **13b**. Molecular weight (M_{wt}) values of the tested members were less than 500. In addition, number of H-bond donors (HBD) and number of H-bond acceptors (HBA) of these compounds are within the accepted values of less than 5 and 10, respectively. Regarding Veber's rule, the number of rotatable bonds and topological polar surface area (TPSA) of such candidates are within the acceptable values of less than 10 and 140 $Å^2$, respectively. These findings conclude that all the tested compounds meet the criteria of Lipinski and Veber's rules and displayed acceptable physicochemical properties.

2.3.2. ADMET profiling study. Utilizing Discovery Studio 4.0,[48–50] the ADMET characteristics of the examined compounds were evaluated (Table 5 and Fig. 3). As a standard drug, thalidomide was used.

Among the tested compounds, **11b**, **13a**, **15a**, **15b**, and **24c** are exhibited low blood–brain barrier (BBB) penetration levels. As a result, it was anticipated that these compounds would not have CNS adverse effects. Regarding aqueous solubility parameters, all compounds showed low to very low levels of aqueous solubility. Next, the intestinal absorption levels of all compounds look like in the good and moderate range. It is interesting to note that compounds **13a,b**, **15a,b**, **19a,b**, and **24a–c** were predicted to not inhibit CYP2D6. As a result, it might

Table 5 ADMET parameters for the tested compounds and thalidomide

Comp	BBB level	Solubility	Absorption	CYP2D6 inhibition	Plasma protein binding
6	0	1	0	True	True
7a	1	1	0	True	True
7b	1	1	0	True	True
11a	0	1	1	True	True
11b	3	1	1	True	True
13a	3	1	0	False	True
13b	0	1	0	False	True
15a	3	2	0	False	False
15b	3	2	0	False	True
19a	2	2	0	False	False
19b	2	2	0	False	False
24a	2	2	0	False	True
24b	2	2	0	False	True
24c	3	2	0	False	True
Thalidomide	3	3	0	False	False

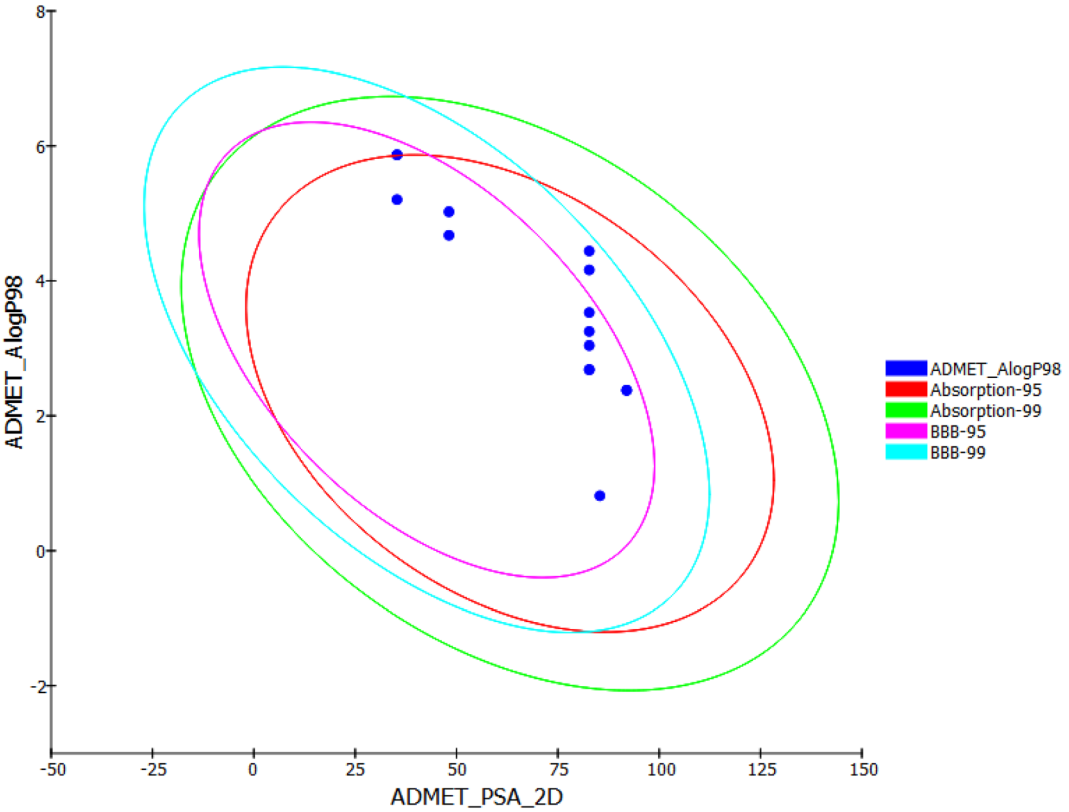

Fig. 3 Computational prediction of ADMET parameters.

be successfully metabolized and eliminated. In terms of plasma protein binding, compounds **15a**, **19a,b** behave similarly to thalidomide in binding in a range of less than 90%. The remainder of compounds, however, was anticipated to bind plasma protein over 90%.

2.3.3. *In silico* toxicity studies. According to the toxicity models created using the Discovery studio software,[51,52] nine toxicity parameters were estimated computationally. Thalidomide was used as a reference (Table 6). For FDA rodent carcinogenicity (rat female) model, all compounds were predicted to

Table 6 *In silico* toxicity studies of the tested compounds and thalidomide

Comp	FDA rodent carcinogenicity (rat-female)	Carcinogenic potency TD_{50} (rat)[a]	Ames mutagenicity	Rat maximum tolerated dose (feed)[b]	Rat Oral LD_{50} [b]	Rat chronic LOAEL[b]	Skin irritancy	Ocular irritancy	DTP
6	Non-carcinogen	18.598	Mutagen	0.106	0.023	0.021	Non-irritant	Mild	Non-toxic
7a	Non-carcinogen	12.040	Mutagen	0.240	0.156	0.022	Non-irritant	Mild	Non-toxic
7b	Non-carcinogen	35.737	Non-mutagen	0.299	0.115	0.020	Non-irritant	Mild	Non-toxic
11a	Non-carcinogen	15.970	Non-mutagen	0.088	0.019	0.013	Non-irritant	Mild	Non-toxic
11b	Non-carcinogen	0.679	Non-mutagen	0.146	0.169	0.037	Non-irritant	Moderate	Non-toxic
13a	Non-carcinogen	11.211	Non-mutagen	0.282	0.064	0.038	Non-irritant	Mild	Non-toxic
13b	Non-carcinogen	6.050	Non-mutagen	0.088	0.008	0.010	Non-irritant	Moderate	Non-toxic
15a	Non-carcinogen	0.257	Non-mutagen	0.146	0.119	0.034	Non-irritant	Moderate	Non-toxic
15b	Non-carcinogen	29.594	Mutagen	0.282	0.091	0.041	Non-irritant	Mild	Non-toxic
19a	Non-carcinogen	10.189	Non-mutagen	0.174	0.924	0.041	Non-irritant	Mild	Non-toxic
19b	Non-carcinogen	12.243	Non-mutagen	0.185	0.139	0.038	Non-irritant	Mild	Toxic
24a	Non-carcinogen	12.655	Non-mutagen	0.204	3.675	0.097	Non-irritant	Mild	Non-toxic
24b	Non-carcinogen	15.153	Non-mutagen	0.217	0.566	0.087	Non-irritant	Mild	Non-toxic
24c	Non-carcinogen	38.125	Non-mutagen	0.246	1.043	0.105	Non-irritant	Mild	Non-toxic
Thalidomide	Carcinogen	26.375	Non-mutagen	0.047	0.835	0.133	Non-irritant	None	Non-toxic

[a] Unit: mg per kg body weight per day. [b] Unit: g per kg body weight.

be non-carcinogenic. For carcinogenic potency TD_{50} rat model, compounds **7b**, **15b**, and **24c** showed TD_{50} values of 35.737, 29.594, and 38.125 mg per kg body weight, which are higher than thalidomide (26.375). For Ames mutagenicity model, all compounds except **6**, **7a**, and **15b** were non-mutagen. Regarding rat maximum tolerated dose model, all compounds demonstrated values higher than that of thalidomide (0.047 g per kg body weight). Additionally, all compounds except **19b** were estimated to be non-toxic against developmental toxicity potential model. For rat oral LD_{50} and model, all compounds except **19a** (0.924 g per kg body weight), **24a** (3.675 g per kg body weight), and **24c** (1.043 g per kg body weight) revealed oral LD_{50} values lower than that of thalidomide (0.835 g per kg body weight). For rat chronic LOAEL model, the tested compounds displayed LOAEL values ranging from 0.010 to 0.105 g per kg body weight. These values are lower than thalidomide (0.133 g per kg body weight). Furthermore, all compounds were non-irritant and mild irritant against skin irritancy and ocular irritancy models, respectively.

3. Conclusion

Fourteen new compounds, based on quinazoline and phthalazine, were designed and synthesized according to the pharmacophoric features of thalidomide in order to get potential immunomodulatory anticancer agents. *N*-phthalazinylbenzenesulfonhydrazide (**24a–c**) emerged as the most potent derivatives in terms of antiproliferative activity. Among which, **24b** was the most significant, showing IC_{50} of 2.51, 5.80 and 4.11 μg mL^{-1} compared to 11.26, 14.58, and 16.87 μg mL^{-1} for thalidomide against HepG-2, MCF-7, and PC3 cell lines respectively. Furthermore, it exhibited immunomodulatory properties, including considerable reduction of the expression levels of TNF-α and NF-κB P65 in HepG-2 cells. Additionally, other biological activities of thalidomide were proven to **24b** such as inhibition of VEGF and caspase-8. Consequently, this work suggests that compound **24b** showed significant biological activity on many targets in a manner similar to thalidomide, and hence it should be considered for further evaluation and modification in order to obtain new potential immunomodulatory anticancer agents.

4. Experimental

4.1. Chemistry

All the reagents, chemicals, and apparatus were described in ESI.† The targeted compounds were furnished following the reported methods.

4.1.1. General procedure for synthesis of the target compound 6. To a solution of 2,4-dichloroquinazoline **4** (1.00 g, 5.02 mmol) and Et_3N (0.87 mL, 6.03 mmol) in isopropanol, 3-chloro-4-fluoroaniline **5** (73) (0.8 g, 5.53 mmol) was added. The reaction mixture was refluxed for 4 h. After the reaction was complete (monitored by TLC), the reaction mixture was cooled to r.t. and poured portion wise to crushed ice while stirring. The obtained precipitate was collected by filtration, washed with water, dried and crystallized from ethanol to furnish the 4-aminoquinazoline derivative **6**.

*4.1.1.1. 2-Chloro-N-(3-chloro-4-fluorophenyl)quinazolin-4-amine **6**.*

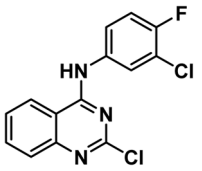

Solid (yield, 77.51%); m.p. = 286–288 °C. IR (KBr, cm^{-1}): 3380 (1NH), 3059 (CH aromatic); ^{1}H NMR (DMSO-*d*6) δ ppm: 10.26 (s, 1H, N**H**), 8.52 (s, 1H, Ar–H), 8.08 (dd, J = 7.2, 2.6 Hz, 1H, Ar–H), 7.90 (dd, J = 8.0, 2.4 Hz, 1H, Ar–H), 7.79 (m, 1H, Ar–H), 7.73 (d, J = 8.4 Hz, 1H, Ar–H), 7.67 (dd, J = 7.8, 2.6 Hz, 1H, Ar–H), 7.49 (d, J = 8.0, 4.2 Hz, 1H, Ar–H); anal. (calcd) for $C_{14}H_8Cl_2FN_3$ (308.14): **C**, 54.57 (54.73); **H**, 2.62 (2.85); **N**, 13.64 (13.81).

4.1.2. General procedure for synthesis of the target compounds 7a,b. To a suspension of 2-chloro-*N*-(3-chloro-4-fluorophenyl)quinazolin-4-amine (**6**) (0.25 g, 0.81 mmol) and Et_3N (0.14 mL, 0.97 mmol) in acetonitrile, an appropriate amine namely; methyl and ethyl amine was added. The reaction mixture was refluxed for 4 h. The reaction mixture was cooled to r.t. and poured portion wise to crushed ice while stirring. The obtained precipitate was collected by filtration, washed, dried and crystallized from ethanol to afford the corresponding 2,4-quinazolinediamine derivatives (**7a,b**), respectively.

*4.1.2.1. N^4-(3-Chloro-4-fluorophenyl)-N^2-methylquinazoline-2,4-diamine **7a**.*

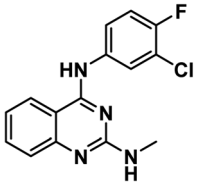

Solid (yield, 85.50%); m.p. = 264–266 °C. IR (KBr, cm^{-1}): 3371, 3277 (2NH), 3125 (CH aromatic), 2954 (CH aliphatic); ^{1}H NMR (DMSO-*d*6) δ ppm: 9.48 (s, 1H, N**H**Ph), 8.30 (s, 1H, N**H**CH_3), 8.25 (s, 1H, Ar–H), 7.93 (dd, J = 8.6, 4.2 Hz, 1H, Ar–H), 7.58 (dd, J = 8.2, 2.6 Hz, 1H, Ar–H), 7.38 (m, 2H, Ar–H), 7.15 (d, J = 7.6 Hz, 1H, Ar–H), 6.83 (m, 1H, Ar–H), 2.87 (d, J = 8.2 Hz, 3H, C**H**$_3$); anal. calcd for $C_{15}H_{12}ClFN_4$ (302.74): **C**, 59.51 (59.38); **H**, 4.00 (4.12); **N**, 18.51 (18.32).

*4.1.2.2. N^4-(3-Chloro-4-fluorophenyl)-N^2-ethylquinazoline-2,4-diamine **7b**.*

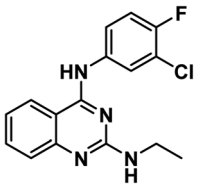

Solid (yield, 85.60%); m.p. = 270–272 °C. IR (KBr, cm^{-1}): 3374, 3217 (2NH), 2979 (CH aliphatic); ^{1}H NMR (DMSO-*d*6) δ ppm:

9.66 (s, 1H, N**H**Ph), 9.20 (s, 1H, N**H**CH_3), 8.36 (s, 1H, Ar–H), 8.13 (d, J = 8.3 Hz, 1H, Ar–H), 8.03 (m, 1H, Ar–H), 7.68 (dd, J = 7.5, 4.6 Hz, 1H, Ar–H), 7.46 (d, J = 8.4 Hz, 1H, Ar–H), 7.33 (m, 2H, Ar–H), 3.48 (m, 2H, $CH_3C\underline{H_2}$), 1.02 (t, J = 7.1 Hz, 3H,$C\underline{H_3}CH_2$); ^{13}C NMR (101 MHz, DMSO-d_6) δ 158.59, 152.19, 137.34, 133.68, 123.43, 122.69, 122.38, 119.35, 119.16, 117.02, 116.81, 38.73, 15.08; mass (m/z): 318 (M^++2), 316 (M^+), and 78 (100%, base peak); anal. calcd for $C_{16}H_{14}ClFN_4$ (316.76): **C**, 60.67 (60.91); **H**, 4.46 (4.42); **N**, 17.69 (17.87).

4.1.3. General procedure for synthesis of the target compounds 11a,b. 3-Chloro-4-fluoroaniline **5** (0.19 g, 1.28 mmol) was added to a mixture of a 2,4,5-trichloroquinazoline **10a** or 2,4,6-trichloroquinazoline **10b** (0.25 g, 1.07 mmol) and Et_3N (0.19 mL, 1.28 mmol) in isopropanol. The reaction mixture was stirred at r.t. for 8 h. The formed solid was collected by filtration, washed and crystallized from ethanol to give the corresponding 4-aminoquinazoline derivatives (**11a,b**), respectively.

*4.1.3.1. 2,5-Dichloro-N-(3-chloro-4-fluorophenyl)quinazolin-4-amine **11a**.*

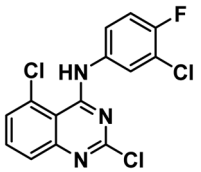

Solid (yield, 81.78%); m.p. = 132–135 °C. IR (KBr, cm^{-1}): 3381 (1NH), 3059 (CH aromatic); ^{1}H NMR (DMSO-$d6$) δ ppm: 9.87 (s, 1H, N**H**), 8.00 (s, 1H, Ar–H), 7.86 (d, J = 8.0 Hz, 1H, Ar–H), 7.73 (m, 3H, Ar–H), 7.52 (dd, J = 6.8, 2.6 Hz, 1H, Ar–H); ^{13}C NMR (101 MHz, DMSO-d_6) δ 158.73, 156.19, 153.85, 134.56, 129.74, 129.08, 127.23, 125.62, 124.50, 124.43, 117.35, 117.13, 111.97; mass (m/z): 343 (M^+ + 1), 342 (M^+), and 157 (100%, base peak). Anal. calcd for $C_{14}H_7C_{l3}FN_3$ (342.58): **C**, 49.08 (49.29); **H**, 2.06 (2.18); **N**, 12.27 (12.49).

*4.1.3.2. 2,6-Dichloro-N-(3-chloro-4-fluorophenyl)quinazolin-4-amine **11b**.*

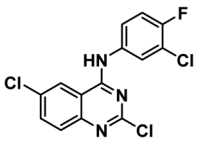

Solid (yield, 79.06%); m.p. = 145–146 °C. IR (KBr, cm^{-1}): 3419 (1NH), 3065 (CH aromatic); ^{1}H NMR (DMSO-$d6$) δ ppm: 10.31 (s, 1H, N**H**), 8.70 (s, 1H, Ar–H), 8.09 (s, 1H, Ar–H), 7.94 (d, J = 8.1 Hz, 1H, Ar–H), 7.79 (m, 2H, Ar–H), 7.52 (dd, J = 6.8, 2.6 Hz, 1H, Ar–H); ^{13}C NMR (101 MHz, DMSO-d_6) δ 158.77, 156.68, 149.91, 134.92, 131.40, 129.49, 124.62, 123.41, 123.34, 123.13, 117.37, 117.15, 115.05; mass (m/z): 343 (M^+ + 1), 342 (M^+), and 100 (100%, base peak). Anal. calcd for $C_{14}H_7C_{l3}FN_3$ (342.58): **C**, 49.08 (49.24); **H**, 2.06 (2.18); **N**, 12.27 (12.44).

4.1.4. General procedure for synthesis of the target compounds 13a,b. A mixture of 2,4,5-trichloroquinazoline **10a** or 2,4,6-trichloroquinazoline **10b** (0.25 g, 1.07 mmol), Et_3N (0.34 mL, 2.36 mmol) and 3-aminopiperidine-2,6-dione hydrochloride **12** (0.19 g, 1.18 mmol) in isopropanol (20 mL) was stirred at r.t. for 8 h. The obtained precipitate was collected by filtration, washed with water, dried and crystallized from ethanol to give the corresponding 4-aminoquinazoline derivatives (**13a,b**), respectively.

*4.1.4.1. 3-((2,5-Dichloroquinazolin-4-yl)amino)piperidine-2,6-dione **13a**.*

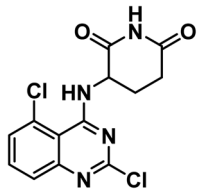

Solid (yield, 51.70%); m.p. = 218–220 °C. IR (KBr, cm^{-1}): 3344, 3195 (2NH), 3088 (CH aromatic), 2855 (CH aliphatic), 1698 (C=O imide); ^{1}H NMR (DMSO-$d6$) δ ppm: 11.04 (s, 1H, CON**H**CO), 8.72 (d, J = 8.1 Hz, 1H, CN**H**CH), 7.76 (m, 1H, Ar–H), 7.63 (m, 2H, Ar–H), 5.07 (m, 1H, C**H**-piperidine), 3.13 (m, 1H, $CH_2C\underline{H_2}$CONH-piperidine), 2.81 (m, 1H, $CH_2C\underline{H_2}$-CONH-piperidine), 2.56 (m, 1H, $C\underline{H_2}CH_2$CONH-piperidine), 2.27 (m, 1H, $C\underline{H_2}CH_2$CONH-piperidine); anal. calcd for $C_{13}H_{10}Cl_2N_4O_2$ (325.15): **C**, 48.02 (48.28); **H**, 3.10 (3.34); **N**, 17.23 (17.41).

*4.1.4.2. 3-((2,6-Dichloroquinazolin-4-yl)amino)piperidine-2,6-dione **13b**.*

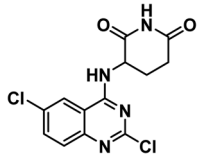

Solid (yield, 45.96%); m.p. = 198–200 °C. IR (KBr, cm^{-1}): 3316, 3186 (2NH), 3093 (CH aromatic), 2875 (CH aliphatic), 1725 (C=O imide); 10.99 (s, 1H, CON**H**CO), 9.02 (d, J = 8.2 Hz, 1H, CN**H**CH), 8.47 (s, 1H, Ar–H), 7.89 (d, J = 8.9 Hz, 1H, Ar–H), 7.71 (d, J = 8.9 Hz, 1H, Ar–H), 5.19 (m, 1H, C**H**-piperidine), 2.90 (m, 1H, $CH_2C\underline{H_2}$CONH-piperidine), 2.62 (m, 1H, $CH_2C\underline{H_2}$CONH-piperidine), 2.25 (m, 1H, $C\underline{H_2}CH_2$CONH-piperidine), 2.11 (m, 1H, $C\underline{H_2}CH_2$CONH-piperidine); ^{13}C NMR (101 MHz, DMSO-d_6) δ 173.38, 171.97, 160.98, 157.32, 149.60, 134.72, 130.91, 129.39, 123.00, 114.76, 51.18, 31.36, 23.95; mass (m/z): 327 (M^+ + 2), 326 (M^+ + 1), 325 (M^+), and 304 (100%, base peak). Anal. calcd for $C_{13}H_{10}Cl_2N_4O_2$ (325.15): **C**, 48.02 (48.25); **H**, 3.10 (3.31); **N**, 17.23 (17.59).

4.1.5. General procedure for synthesis of the target compounds 15a,b. A mixture of 2,4,5-trichloroquinazoline or 2,4,6-trichloroquinazoline (0.25 g, 1.07 mmol), Et_3N (0.19 mL, 1.28 mmol) and semicarbazide (0.01 g, 1.28 mmol) in isopropanol (20 mL) was stirred at r.t. for 8 h. After the reaction was complete (monitored by TLC), the obtained precipitate was collected by filtration, washed with water, dried and crystallized from ethanol to give the corresponding 4-aminoquinazoline derivatives (VIII$_{a\text{-}b}$), respectively.

*4.1.5.1. 2-(2,5-Dichloroquinazolin-4-yl)hydrazine-1-carboxamide **15a**.*

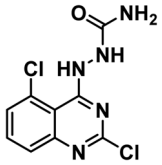

Solid (yield, 75.51%); m.p. = 189–191 °C. IR (KBr, cm^{-1}): 3457, 3349, 3274, 3194 (br, 4NH), 3050 (CH aromatic); ^{1}H NMR (DMSO-*d*6) δ ppm: 9.87 (s, 1H, NHN**H**CO), 8.53 (s, 1H, N**H**NHCO), 7.70 (d, J = 8.2 Hz, 1H, Ar–H), 7.56 (d, J = 8.00 Hz, 1H, Ar–H), 7.45 (m, 1H, Ar–H), 6.25 (s, 2H, N**H$_2$**); anal. calcd for $C_9H_7Cl_2N_5O$ (272.09): **C**, 39.73 (39.88); **H**, 2.59 (2.75); **N**, 25.74 (25.53).

*4.1.5.2. 2-(2,6-Dichloroquinazolin-4-yl)hydrazine-1-carboxamide **15b**.*

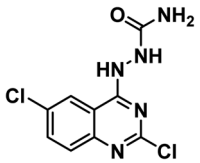

Solid (yield, 68.65%); m.p. = 171–173 °C. IR (KBr, cm^{-1}): 3471, 3426, 3267, 3190 (br, 4NH), 3027 (CH aromatic); ^{1}H NMR (DMSO-*d*6) δ ppm: 10.43 (s, 1H, NHN**H**CO), 8.45 (s, 1H, N**H**NHCO),8.24 (d, J = 8.2 Hz, 1H, Ar–H), 7.88 (d, J = 8.4 Hz, 1H, Ar–H), 7.72 (m, 1H, Ar–H), 6.20 (s, 2H, N**H$_2$**); ^{13}C NMR (101 MHz, DMSO-d_6) δ 161.90, 157.71, 134.74, 130.83, 129.18, 123.26, 113.78; mass (*m*/*z*): 274 (M^+ + 2), 272 (M^+), and 127 (100%, base peak); anal. calcd for $C_9H_7Cl_2N_5O$ (272.09): C, 39.73 (39.90); H, 2.59 (2.78); N, 25.74 (25.91).

4.1.6. General procedure for synthesis of the target compounds 19a,b. To a mixture of 2,5-dichloro-4-hydrazinylquinazoline (**17**) (0.25 g, 1.09 mmol) and Et_3N (0.19 mL, 1.31 mmol) in DMF, an appropriate benzenesulfonyl chloride (1.20 mmol) namely; 4-methylbenzenesulfonyl chloride **18a** and 4-fluorobenzenesulfonyl chloride **18b** was added dropwise in ice salt bath. The reaction mixture was stirred for 2 h. The reaction mixture was poured into crushed ice to give a precipitate. The formed precipitate was collected by filtration, washed with water, dried and crystallized from ethanol to afford the corresponding benzenesulfonohydrazide derivatives (**19a,b**), respectively.

*4.1.6.1. N′-(2,5-Dichloroquinazolin-4-yl)-4-methylbenzenesulfonohydrazide **19a**.*

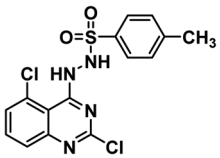

Solid (yield, 83.68%); m.p. = 155–157 °C. IR (KBr, cm^{-1}): 3397, 3306 (2NH), 3086 (CH aromatic), 1163 (SO_2 group); ^{1}H NMR (DMSO-*d*6) δ ppm: 10.04 (s, 1H, NHN**H**SO_2), 7.82 (s, 1H, N**H**NHSO_2), 7.78 (s, 1H, Ar–H), 7.70 (d, J = 8.4 Hz, 1H, Ar–H), 7.64 (d, J = 8.3 Hz, 1H, Ar–H), 7.53 (d, J = 8.2 Hz, 1H, Ar–H), 7.46 (m, 1H, Ar–H), 7.33 (d, J = 8.0 Hz, 2H, Ar–H), 2.31 (s, 3H, C**H$_3$**); anal. calcd for $C_{15}H_{12}Cl_2N_4O_2S$ (383.25): **C**, 47.01 (47.27); **H**, 3.16 (3.38); **N**, 14.62 (14.89).

*4.1.6.2. N′-(2,5-Dichloroquinazolin-4-yl)-4-fluorobenzenesulfonohydrazide **19b**.*

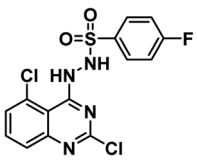

Solid (yield, 66.26%); m.p. = 168–170 °C. IR (KBr, cm^{-1}): 3396, 3306 (2NH), 3065 (CH aromatic), 1166 (SO_2 group); ^{1}H NMR (DMSO-*d*6) δ ppm: 10.24 (s, 1H, NHN**H**SO_2), 7.97 (s, 1H, N**H**NHSO_2), 7.95 (s, 1H, Ar–H), 7.69 (m, 2H, Ar–H), 7.64 (d, J = 8.3 Hz, 1H, Ar–H), 7.53 (d, J = 8.2 Hz, 1H, Ar–H), 7.39 (m, 2H, Ar–H); ^{13}C NMR (101 MHz, DMSO-d_6) δ 163.69, 146.43, 144.82, 135.62, 133.76, 133.42, 131.41, 129.66, 129.57, 126.21, 116.52, 116.30, 115.42, 103.97; mass (*m*/*z*): 389 (M^++2), 387 (M^+), and 193 (100%, base peak); anal. calcd for $C_{14}H_9Cl_2FN_4O_2S$ (387.21): **C**, 43.43 (43.54); **H**, 2.34 (2.50); **N**, 14.47 (14.63).

4.1.7. General procedure for synthesis of the target compounds 24a–c. To a solution of 1-chloro-4-hydrazinylphthalazine **23** (0.25 g, 1.28 mmol) and E_3N (0.22 mL, 1.54 mmol) in DMF, an appropriate benzenesulfonyl chloride (1.41 mmol) namely; 4-methylbenzene sulfonyl chloride, 4-fluorobenzenesulfonyl chloride and benzenesulfonyl chloride, was added dropwise. The reaction mixture was stirred in ice salt bath for 1 h. After the reaction was complete (monitored by TLC), the reaction mixture was cooled to room temperature and poured portion wise to crushed ice while stirring. The formed solid was collected by filtration, washed, dried and crystallized from ethanol to give the corresponding benzenesulfonohydrazide derivatives **24a–c** respectively.

*4.1.7.1. N′-(4-Chlorophthalazin-1-yl)-4-methylbenzenesulfonohydrazide **24a**.*

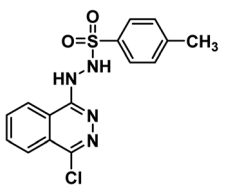

Solid (yield, 80.35%); m.p. = 235–237 °C. IR (KBr, cm^{-1}): 3330, 3188 (2NH), 3062 (CH aromatic), 2921 (CH aliphatic), 1166 (SO_2 group); ^{1}H NMR (DMSO-*d*6) δ ppm: 11.72 (s, 1H, N**H**SO_2), 9.24 (s, 1H, CN**H**NH), 7.98 (d, J = 7.8 Hz, 1H, Ar–H), 7.83 (s, 1H, Ar–H), 7.79 (m, 4H, Ar–H), 7.42 (d, J = 7.9 Hz, 2H, Ar–H), 2.40 (s, 3H, C**H$_3$**); anal. calcd for $C_{15}H_{13}ClN_4O_2S$ (348.81): **C**, 51.65 (51.89); **H**, 3.76 (3.85); **N**, 16.06 (16.32).

*4.1.7.2. N′-(4-Chlorophthalazin-1-yl)-4-fluorobenzenesulfonohydrazide **24b**.*

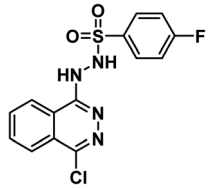

Solid (yield, 83.71%); m.p. = 220–222 °C. IR (KBr, cm^{-1}): 3334, 3189 (2H), 3067 (CH aromatic); ^{1}H NMR (DMSO-*d*6) δ ppm: 11.83 (s, 1H, N**H**SO_2), 9.33 (s, 1H, CN**H**NH), 8.00 (dd, J = 8.00, 4.4 Hz, 3H, Ar–H), 7.77 (m, 3H, Ar–H), 7.47 (m, 2H, Ar–H); anal. calcd for $C_{14}H_{10}ClFN_4O_2S$ (352.77): **C**, 47.67 (47.85); **H**, 2.86 (2.97); **N**, 15.88 (15.62).

*4.1.7.3. N′-(4-Chlorophthalazin-1-yl)benzenesulfonohydrazide **24c**.*

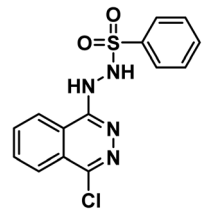

Solid (yield, 77.24%); m.p. = 192–194 °C. IR (KBr, cm^{-1}): 3331, 3199 (2NH), 3063 (CH aromatic); ^{1}H NMR (DMSO-*d*6) δ ppm: 11.75 (s, 1H, N**H**SO_2), 9.44 (s, 1H, CN**H**NH), 8.04 (s, 1H, Ar–H), 7.92 (d, J = 7.6 Hz, 2H, Ar–H), 7.85 (s, 3H, Ar–H), 7.65 (d, J = 7.2 Hz, 1H, Ar–H), 7.61 (d, J = 7.5 Hz, 2H, Ar–H); anal. calcd for $C_{14}H_{11}ClN_4O_2S$ (334.78): **C**, 50.23 (50.34); **H**, 3.31 (3.45); **N**, 16.74 (16.90).

4.2. Biological testing

4.2.1. *In vitro* antitumor assay. This test was carried out on three different human cancer cell lines: MCF-7, HCT116, and HepG2 using the MTT method[53] as described in ESI.†

4.2.2. Estimation of TNF-α, CASP8, and VEGF in HepG-2 cells supernatant. The levels of TNF-α, CASP8, and VEGF in cell culture supernatants were estimated by ELISA technique using commercially available matched paired antibodies (R&D Systems Inc., Minneapolis, MN) according to reported procedure[54,55] as described in ESI.†

4.2.3. Estimation of nuclear factor kappa-B P65 (NF-κB P65) in HepG-2 cell lysate. Anti-rabbit NF-κB P65 polyclonal antibody was measured using the ELISA plate reader in cell lysate[14] as described in ESI.†

4.2.4. Cytotoxicity against Vero cell line. This test was carried out using MTT method on Vero cell line as described in ESI.†[56]

4.2.5. *In silico* studies

4.2.5.1. Pharmacokinetic profiling study. This study was applied using Discover studio 4 (ref. 57) in accordance with the comprehensive description in ESI.†

4.2.5.2. ADMET studies. ADMET descriptors were determined using Discovery studio 4.0 as according to the reported method[58–61] (ESI†).

4.2.5.3. Toxicity studies. The toxicity parameters of the synthesized compounds were calculated using Discovery studio 4.0 as described[62–65] in ESI.†

Conflicts of interest

There is no conflict of interest.

Acknowledgements

This paper is based upon work supported by Science, Technology & Innovation Funding Authority (STIFA) under grant number 43040.

References

1 A. E. Abdallah, R. R. Mabrouk, M. R. Elnagar, A. M. Farrag, M. H. Kalaba, M. H. Sharaf, E. M. El-Fakharany, D. A. Bakhotmah, E. B. Elkaeed and M. M. S. Al Ward, New Series of VEGFR-2 Inhibitors and Apoptosis Enhancers: Design, Synthesis and Biological Evaluation, *Drug Des., Dev. Ther.*, 2022, **16**, 587.

2 A.-M. Florea and D. Büsselberg, Cisplatin as an anti-tumor drug: cellular mechanisms of activity, drug resistance and induced side effects, *Cancers*, 2011, **3**(1), 1351–1371.

3 M. Nikolaou, A. Pavlopoulou, A. G. Georgakilas and E. Kyrodimos, The challenge of drug resistance in cancer treatment: a current overview, *Clin. Exp. Metastasis*, 2018, **35**(4), 309–318.

4 N. Chatterjee and T. G. Bivona, Polytherapy and targeted cancer drug resistance, *Trends Cancer*, 2019, **5**(3), 170–182.

5 J. A. Simon, P. Szankasi, D. K. Nguyen, C. Ludlow, H. M. Dunstan, C. J. Roberts, E. L. Jensen, L. H. Hartwell and S. H. Friend, Differential toxicities of anticancer agents among DNA repair and checkpoint mutants of Saccharomyces cerevisiae, *Cancer Res.*, 2000, **60**(2), 328–333.

6 S. Eckhardt, Recent progress in the development of anticancer agents, *Curr. Med. Chem.: Anti-Cancer Agents*, 2002, **2**(3), 419–439.

7 A. Colombo, C. Cipolla, M. Beggiato and D. Cardinale, Cardiac toxicity of anticancer agents, *Curr. Cardiol. Rep.*, 2013, **15**(5), 1–11.

8 A. Iliadis and D. Barbolosi, Optimizing drug regimens in cancer chemotherapy by an efficacy–toxicity mathematical model, *Comput. Biomed. Res.*, 2000, **33**(3), 211–226.

9 H. Elkady, A. Elwan, H. A. El-Mahdy, A. S. Doghish, A. Ismail, M. S. Taghour, E. B. Elkaeed, I. H. Eissa, M. A. Dahab and H. A. Mahdy, New benzoxazole derivatives as potential VEGFR-2 inhibitors and apoptosis inducers: design, synthesis, anti-proliferative evaluation, flowcytometric analysis, and in silico studies, *J. Enzyme Inhib. Med. Chem.*, 2022, **37**(1), 403–416.

10 M. B. Steins, T. Padró, R. Bieker, S. Ruiz, M. Kropff, J. Kienast, T. Kessler, T. Buechner, W. E. Berdel and R. M. Mesters, Efficacy and safety of thalidomide in patients with acute myeloid leukemia, *Blood*, 2002, **99**(3), 834–839.

11 Y. X. Zhu, K. M. Kortuem and A. K. Stewart, Molecular mechanism of action of immune-modulatory drugs thalidomide, lenalidomide and pomalidomide in multiple myeloma, *Leuk. Lymphoma*, 2013, **54**(4), 683–687.

12 C. Galustian, B. Meyer, M.-C. Labarthe, K. Dredge, D. Klaschka, J. Henry, S. Todryk, R. Chen, G. Muller and D. Stirling, The anti-cancer agents lenalidomide and pomalidomide inhibit the proliferation and function of T regulatory cells, *Cancer Immunol. Immunother.*, 2009, **58**(7), 1033–1045.

13 G. Görgün, E. Calabrese, E. Soydan, T. Hideshima, G. Perrone, M. Bandi, D. Cirstea, L. Santo, Y. Hu and Y.-T. Tai, Immunomodulatory effects of lenalidomide and pomalidomide on interaction of tumor and bone marrow accessory cells in multiple myeloma, *Blood*, 2010, **116**(17), 3227–3237.

14 M. A. El-Zahabi, H. Sakr, K. El-Adl, M. Zayed, A. S. Abdelraheem, S. I. Eissa, H. Elkady and I. H. Eissa, Design, synthesis, and biological evaluation of new challenging thalidomide analogs as potential anticancer immunomodulatory agents, *Bioorg. Chem.*, 2020, **104**, 104218.

15 K. C. Anderson, Lenalidomide and thalidomide: mechanisms of action—similarities and differences, in *Seminars in Hematology*, Elsevier, 2005, pp. S3–S8.

16 S. Kumar and S. V. Rajkumar, Thalidomide and lenalidomide in the treatment of multiple myeloma, *Eur. J. Cancer*, 2006, **42**(11), 1612–1622.

17 S. Lindner and J. Krönke, The molecular mechanism of thalidomide analogs in hematologic malignancies, *J. Mol. Med.*, 2016, **94**(12), 1327–1334.

18 T. Ito and H. Handa, Molecular mechanisms of thalidomide and its derivatives, *Proc. Jpn Acad., Ser. B*, 2020, **96**(6), 189–203.

19 T. Reske, M. Fulciniti and N. C. Munshi, Mechanism of action of immunomodulatory agents in multiple myeloma, *Med. Oncol.*, 2010, **27**(1), 7–13.

20 D. Millrine and T. Kishimoto, A brighter side to thalidomide: its potential use in immunological disorders, *Trends Mol. Med.*, 2017, **23**(4), 348–361.

21 J. Cortés-Hernández, M. Torres-Salido, J. Castro-Marrero, M. Vilardell-Tarres and J. Ordi-Ros, Thalidomide in the treatment of refractory cutaneous lupus erythematosus: prognostic factors of clinical outcome, *Br. J. Dermatol.*, 2012, **166**(3), 616–623.

22 A. Lopez-Girona, D. Mendy, T. Ito, K. Miller, A. Gandhi, J. Kang, S. Karasawa, G. Carmel, P. Jackson and M. Abbasian, Cereblon is a direct protein target for immunomodulatory and antiproliferative activities of lenalidomide and pomalidomide, *Leukemia*, 2012, **26**(11), 2326–2335.

23 P. R. Hagner, H.-W. Man, C. Fontanillo, M. Wang, S. Couto, M. Breider, C. Bjorklund, C. G. Havens, G. Lu and E. Rychak, CC-122, a pleiotropic pathway modifier, mimics an interferon response and has antitumor activity in DLBCL, *Blood*, 2015, **126**(6), 779–789.

24 G. E. Diggle, Thalidomide: 40 years on, *Int. J. Clin. Pract.*, 2001, **55**(9), 627–631.

25 A. K. Akobeng and P. C. Stokkers, Thalidomide and thalidomide analogues for maintenance of remission in Crohn's disease, *Cochrane Database Syst. Rev.*, 2009, (2), CD007350.

26 M. Attal, V. Lauwers-Cances, G. Marit, D. Caillot, P. Moreau, T. Facon, A. M. Stoppa, C. Hulin, L. Benboubker and L. Garderet, Lenalidomide maintenance after stem-cell transplantation for multiple myeloma, *N. Engl. J. Med.*, 2012, **366**(19), 1782–1791.

27 C. Galustian and A. Dalgleish, *Google-2 is logged in Drugs of the Future*, 2011, vol. 36, 10, p. 741, ISSN 0377-8282 Copyright 2011 Prous Science CCC: 0377-8282.

28 M. Offidani, L. Corvatta, P. Caraffa, P. Leoni, C. Pautasso, A. Larocca and A. Palumbo, Pomalidomide for the treatment of relapsed–refractory multiple myeloma: a review of biological and clinical data, *Expert Rev. Anticancer Ther.*, 2014, **14**(5), 499–510.

29 P. Hagner, M. Wang, S. Couto, M. Breider, C. Fontanillo, M. Trotter, C. C. Bjorklund, C. G. Havens, H. K. Raymon and R. K. Narla, CC-122 has potent anti-lymphoma activity through destruction of the Aiolos and Ikaros transcription factors and induction of interferon response pathways, *Blood*, 2014, **124**(21), 3035.

30 A. Renneville, J. A. Gasser, D. E. Grinshpun, P. M. Jean Beltran, N. D. Udeshi, M. E. Matyskiela, T. Clayton, M. McConkey, K. Viswanathan and A. Tepper, Avadomide Induces Degradation of ZMYM2 Fusion Oncoproteins in Hematologic MalignanciesAvadomide Induces ZMYM2 Fusion Oncoprotein Degradation, *Blood Cancer Discovery*, 2021, **2**(3), 250–265.

31 L. Xu and W. A. Russu, Molecular docking and synthesis of novel quinazoline analogues as inhibitors of transcription factors NF-κB activation and their anti-cancer activities, *Bioorg. Med. Chem.*, 2013, **21**(2), 540–546.

32 N.-C. Cho, J. H. Cha, H. Kim, J. Kwak, D. Kim, S.-H. Seo, J.-S. Shin, T. Kim, K. D. Park and J. Lee, Discovery of 2-aryloxy-4-amino-quinazoline derivatives as novel protease-activated receptor 2 (PAR2) antagonists, *Bioorg. Med. Chem.*, 2015, **23**(24), 7717–7727.

33 J. Hu, Y. Zhang, L. Dong, Z. Wang, L. Chen, D. Liang, D. Shi, X. Shan and G. Liang, Design, synthesis, and biological evaluation of novel quinazoline derivatives as anti-inflammatory agents against lipopolysaccharide-induced acute lung injury in rats, *Chem. Biol. Drug Des.*, 2015, **85**(6), 672–684.

34 Y. Pu, D. Cao, C. Xie, H. Pei, D. Li, M. Tang and L. Chen, Anti-arthritis effect of a novel quinazoline derivative through inhibiting production of TNF-α mediated by TNF-α converting enzyme in murine collagen-induced arthritis model, *Biochem. Biophys. Res. Commun.*, 2015, **462**(4), 288–293.

35 A. E. Abdallah, S. I. Eissa, M. M. S. Al Ward, R. R. Mabrouk, A. B. Mehany and M. A. El-Zahabi, Design, synthesis and molecular modeling of new quinazolin-4 (3H)-one based

VEGFR-2 kinase inhibitors for potential anticancer evaluation, *Bioorg. Chem.*, 2021, **109**, 104695.

36 G. A. Bennett, L. A. Radov, L. A. Trusso and V. S. Georgiev, Synthesis and immunomodulating activity of 5H-thiazolo [2,3-b] quinazolin-3 (2H)-one, *J. Pharm. Sci.*, 1987, **76**(8), 633–634.

37 A. E. Abdallah, R. R. Mabrouk, M. M. S. Al Ward, S. I. Eissa, E. B. Elkaeed, A. B. Mehany, M. A. Abo-Saif, O. A. El-Feky, M. S. Alesawy and M. A. El-Zahabi, Synthesis, biological evaluation, and molecular docking of new series of antitumor and apoptosis inducers designed as VEGFR-2 inhibitors, *J. Enzyme Inhib. Med. Chem.*, 2022, **37**(1), 573–591.

38 D.-C. Liu, G.-H. Gong, C.-X. Wei, X.-J. Jin and Z.-S. Quan, Synthesis and anti-inflammatory activity evaluation of a novel series of 6-phenoxy-[1, 2, 4] triazolo [3, 4-a] phthalazine-3-carboxamide derivatives, *Bioorg. Med. Chem. Lett.*, 2016, **26**(6), 1576–1579.

39 K. K. To, D. C. Poon, Y. Wei, F. Wang, G. Lin and L.-w. Fu, Data showing the circumvention of oxaliplatin resistance by vatalanib in colon cancer, *Data Brief*, 2016, **7**, 437–444.

40 D.-Q. Xue, X.-Y. Zhang, C.-J. Wang, L.-Y. Ma, N. Zhu, P. He, K.-P. Shao, P.-J. Chen, Y.-F. Gu and X.-S. Zhang, Synthesis and anticancer activities of novel 1, 2, 4-triazolo [3, 4-a] phthalazine derivatives, *Eur. J. Med. Chem.*, 2014, **85**, 235–244.

41 W. M. Eldehna, S. M. Abou-Seri, A. M. El Kerdawy, R. R. Ayyad, A. M. Hamdy, H. A. Ghabbour, M. M. Ali and D. A. Abou El Ella, Increasing the binding affinity of VEGFR-2 inhibitors by extending their hydrophobic interaction with the active site: Design, synthesis and biological evaluation of 1-substituted-4-(4-methoxybenzyl) phthalazine derivatives, *Eur. J. Med. Chem.*, 2016, **113**, 50–62.

42 N. Jiang, X. Zhai, Y. Zhao, Y. Liu, B. Qi, H. Tao and P. Gong, Synthesis and biological evaluation of novel 2-(2-arylmethylene) hydrazinyl-4-aminoquinazoline derivatives as potent antitumor agents, *Eur. J. Med. Chem.*, 2012, **54**, 534–541.

43 D. Shah, H. Lakum and K. Chikhalia, Synthesis and in vitro antimicrobial evaluation of piperazine substituted quinazoline-based thiourea/thiazolidinone/chalcone hybrids, *Russ. J. Bioorg. Chem.*, 2015, **41**(2), 209–222.

44 K. S. Van Horn, X. Zhu, T. Pandharkar, S. Yang, B. Vesely, M. Vanaerschot, J.-C. Dujardin, S. Rijal, D. E. Kyle and M. Z. Wang, Antileishmanial activity of a series of N 2, N 4-disubstituted quinazoline-2, 4-diamines, *J. Med. Chem.*, 2014, **57**(12), 5141–5156.

45 M. M. Gineinah, M. A. El-Sherbeny, M. N. Nasr and A. R. Maarouf, Synthesis and Antiinflammatory Screening of Some Quinazoline and Quinazolyl-4-oxoquinazoline Derivatives, *Arch. Pharm.*, 2002, **335**(11–12), 556–562.

46 H. Drew and R. Garwood, 177. Chemiluminescent organic compounds. Part VII. Substituted phthalaz-1: 4-diones. Effect of substituents on the luminescent power, *J. Chem. Soc.*, 1939, 836–837.

47 J. C. Pritchett, L. Naesens and J. Montoya, *Treating HHV-6 infections: The laboratory efficacy and clinical use of ati-HHV-6 agents*, 2014.

48 N. A. Alsaif, M. A. Dahab, M. M. Alanazi, A. J. Obaidullah, A. A. Al-Mehizia, M. M. Alanazi, S. Aldawas, H. A. Mahdy and H. Elkady, New quinoxaline derivatives as VEGFR-2 inhibitors with anticancer and apoptotic activity: design, molecular modeling, and synthesis, *Bioorg. Chem.*, 2021, **110**, 104807.

49 S. A. El-Metwally, M. M. Abou-El-Regal, I. H. Eissa, A. B. Mehany, H. A. Mahdy, H. Elkady, A. Elwan and E. B. Elkaeed, Discovery of thieno [2, 3-d] pyrimidine-based derivatives as potent VEGFR-2 kinase inhibitors and anticancer agents, *Bioorg. Chem.*, 2021, **112**, 104947.

50 N. A. Alsaif, M. S. Taghour, M. M. Alanazi, A. J. Obaidullah, A. A. Al-Mehizia, M. M. Alanazi, S. Aldawas, A. Elwan and H. Elkady, Discovery of new VEGFR-2 inhibitors based on bis ([1, 2, 4] triazolo)[4, 3-a: 3', 4'-c] quinoxaline derivatives as anticancer agents and apoptosis inducers, *J. Enzyme Inhib. Med. Chem.*, 2021, **36**(1), 1093–1114.

51 M. M. Alanazi, I. H. Eissa, N. A. Alsaif, A. J. Obaidullah, W. A. Alanazi, A. F. Alasmari, H. Albassam, H. Elkady and A. Elwan, Design, synthesis, docking, ADMET studies, and anticancer evaluation of new 3-methylquinoxaline derivatives as VEGFR-2 inhibitors and apoptosis inducers, *J. Enzyme Inhib. Med. Chem.*, 2021, **36**(1), 1760–1782.

52 M. S. Taghour, H. A. Mahdy, M. H. Gomaa, A. Aglan, M. G. Eldeib, A. Elwan, M. A. Dahab, E. B. Elkaeed, A. A. Alsfouk and M. M. Khalifa, Benzoxazole derivatives as new VEGFR-2 inhibitors and apoptosis inducers: design, synthesis, in silico studies, and antiproliferative evaluation, *J. Enzyme Inhib. Med. Chem.*, 2022, **37**(1), 2063–2077.

53 D. Gerlier and N. Thomasset, Use of MTT colorimetric assay to measure cell activation, *J. Immunol. Methods*, 1986, **94**(1–2), 57–63.

54 R. M. Talaat, Soluble angiogenesis factors in sera of Egyptian patients with hepatitis C virus infection: correlation with disease severity, *Viral Immunol.*, 2010, **23**(2), 151–157.

55 *MyBioSource ELISA Test Kits*, **https://www.mybiosource.com/human-elisa-kits/casp8/2513072#QLAPP_MBS2513072_TD**.

56 M. S. Taghour, H. Elkady, W. M. Eldehna, N. El-Deeb, A. M. Kenawy, E. B. Elkaeed, B. A. Alsfouk, M. S. Alesawy, D. Z. Husein and A. M. Metwaly, Design, synthesis, antiproliferative evaluation, docking, and MD simulations studies of new thiazolidine-2, 4-diones targeting VEGFR-2 and apoptosis pathway, *PLoS One*, 2022, **17**(9), e0272362.

57 A. Belal, H. Elkady, A. A. Al-Karmalawy, A. H. Amin, M. M. Ghoneim, M. El-Sherbiny, R. H. Al-Serwi, M. A. Abdou, M. H. Ibrahim and A. Mehany, Discovery of Some Heterocyclic Molecules as Bone Morphogenetic Protein 2 (BMP-2)-Inducible Kinase Inhibitors: Virtual Screening, ADME Properties, and Molecular Docking Simulations, *Molecules*, 2022, **27**(17), 5571.

58 E. B. Elkaeed, R. G. Yousef, H. Elkady, I. M. Gobaara, A. A. Alsfouk, D. Z. Husein, I. M. Ibrahim, A. M. Metwaly and I. H. Eissa, The Assessment of Anticancer and VEGFR-2 Inhibitory Activities of a New 1H-Indole Derivative: In Silico and In Vitro Approaches, *Processes*, 2022, **10**(7), 1391.

59 E. B. Elkaeed, R. G. Yousef, H. Elkady, I. M. Gobaara, B. A. Alsfouk, D. Z. Husein, I. M. Ibrahim, A. M. Metwaly and I. H. Eissa, Design, synthesis, docking, DFT, MD simulation studies of a new nicotinamide-based derivative: In vitro anticancer and VEGFR-2 inhibitory effects, *Molecules*, 2022, **27**(14), 4606.

60 E. B. Elkaeed, I. H. Eissa, H. Elkady, A. Abdelalim, A. M. Alqaisi, A. A. Alsfouk, A. Elwan and A. M. Metwaly, A Multistage In Silico Study of Natural Potential Inhibitors Targeting SARS-CoV-2 Main Protease, *Int. J. Mol. Sci.*, 2022, **23**(15), 8407.

61 E. B. Elkaeed, F. S. Youssef, I. H. Eissa, H. Elkady, A. A. Alsfouk, M. L. Ashour, M. A. El Hassab and S. M. Abou-Seri, Metwaly AM: Multi-Step In Silico Discovery of Natural Drugs against COVID-19 Targeting Main Protease, *Int. J. Mol. Sci.*, 2022, **23**(13), 6912.

62 M. S. Taghour, H. Elkady, W. M. Eldehna, N. M. El-Deeb, A. M. Kenawy, E. B. Elkaeed, A. A. Alsfouk, M. S. Alesawy, A. M. Metwaly and I. H. Eissa, Design and synthesis of thiazolidine-2, 4-diones hybrids with 1, 2-dihydroquinolones and 2-oxindoles as potential VEGFR-2 inhibitors: in-vitro anticancer evaluation and in-silico studies, *J. Enzyme Inhib. Med. Chem.*, 2022, **37**(1), 1903–1917.

63 A. Belal, N. M. Abdel Gawad, A. B. Mehany, M. A. Abourehab, H. Elkady, A. A. Al-Karmalawy and A. S. Ismael, Design, synthesis and molecular docking of new fused 1 H-pyrroles, pyrrolo [3, 2-d] pyrimidines and pyrrolo [3, 2-e][1, 4] diazepine derivatives as potent EGFR/CDK2 inhibitors, *J. Enzyme Inhib. Med. Chem.*, 2022, **37**(1), 1884–1902.

64 M. M. Alanazi, H. Elkady, N. A. Alsaif, A. J. Obaidullah, H. M. Alkahtani, M. M. Alanazi, M. A. Alharbi, I. H. Eissa and M. A. Dahab, New quinoxaline-based VEGFR-2 inhibitors: design, synthesis, and antiproliferative evaluation with in silico docking, ADMET, toxicity, and DFT studies, *RSC Adv.*, 2021, **11**(48), 30315–30328.

65 M. M. Alanazi, H. Elkady, N. A. Alsaif, A. J. Obaidullah, W. A. Alanazi, A. M. Al-Hossaini, M. A. Alharbi, I. H. Eissa and M. A. Dahab, Discovery of new quinoxaline-based derivatives as anticancer agents and potent VEGFR-2 inhibitors: Design, synthesis, and in silico study, *J. Mol. Struct.*, 2021, 132220.